2012

Quantum theory of longitudinal momentum transfer in above-threshold ionization

A. S. Titi

Gordon W. F. Drake
University of Windsor

PHYSICAL REVIEW A **85**, 041404(R) (2012)

Quantum theory of longitudinal momentum transfer in above-threshold ionization

A. S. Titi* and G. W. F. Drake†
Department of Physics, University of Windsor, Windsor, Ontario, Canada N9B 3P4
(Received 29 January 2012; published 23 April 2012)

In the ionization process, longitudinal momentum along the direction of propagation is transferred to the photoelectrons due to the action of the magnetic component of Lorentz force. In a recent experiment by Smeenk *et al*. [Phys. Rev. Lett. **106**, 193002 (2011)], such a transfer is observed in the ionization of argon and neon atoms by circularly polarized light at 800 and 1400 nm in the intensity range of 10^{14}–10^{15} W/cm^2. They accounted for the results by a purely classical model. We present a fully quantum-mechanical calculation of the transfer of longitudinal momentum to the photoelectrons. The results are in agreement with the observations of Smeenk *et al*. at high intensities, but clear evidence for additional Coulomb interactions emerges at low intensities.

DOI: 10.1103/PhysRevA.85.041404 PACS number(s): 32.80.Rm, 32.80.Wr

In the multiphoton ionization of atoms by a strong light field, several photons are absorbed, resulting in the transfer of the photon energy, linear and angular momenta to the electron-ion system. Due to the smallness of the linear momentum of a single visible photon, it is usually neglected. Recently, however, the transfer of the photon linear momentum was clearly observed in the experiment of Smeenk *et al*. [1]. It is also known that a large number of photons can produce the macroscopic effect of radiation pressure [2,3]. Recently, the photon linear momentum transfer to the photoelectron, i.e., radiation pressure, has been invoked to account for the generation of terahertz radiation emitted by laser-generated filaments [4–6]. Motivated by the observations of Smeenk *et al*. [1], we present within the single active electron approximation, a theoretical formulation for the simultaneous transfer of both the photon linear and the angular momentum in the ionization process. We then restrict attention to the transfer of photon linear momentum.

In the dipole approximation, the expression $e^{i\mathbf{k}\cdot\mathbf{r}} = 1 + i\mathbf{k}\cdot\mathbf{r} + \cdots$ is replaced by unity when the radiation wavelength is large compared with a length characteristic of the system. Here, $\mathbf{k}$ is the radiation-field propagation vector. This makes the vector potential $\mathbf{A}$ space independent. To obtain longitudinal momentum transfer effects, a nondipole formulation is required. We start with the exact expression for the time-reversed transition amplitude from a ground state $\phi_{\rm i}$ to a final continuum state $\Psi_{\rm f}^-$ [7] (atomic units are used throughout),

$$(S-1)_{\rm fi} = -i\int_{-\infty}^{\infty} dt \langle \Psi_{\rm f}^- | V_{\rm L} \phi_{\rm i}\rangle. \tag{1}$$

The final state $\Psi_{\rm f}^-$ is the solution of the time-dependent Schrödinger equation for an atomic electron interacting with a laser field,

$$(i\partial_{\rm t} - H_0 - V_{\rm L} - V_{\rm A})\Psi_{\rm f}^-(\mathbf{r},t) = 0. \tag{2}$$

Here, H_0 is the free Hamiltonian, $V_{\rm A}$ is the atomic Coulomb potential, and $V_{\rm L} = \frac{1}{c}\mathbf{A}(\varphi)\cdot\hat{\mathbf{P}} + \frac{A(\varphi)^2}{2c^2}$ is the atom-laser interaction Hamiltonian where $\hat{\mathbf{P}} = -i\nabla$ is the momentum operator and $\mathbf{A} = \mathbf{A}(\varphi)$ with $\varphi = \mathbf{k}\cdot\mathbf{r} - \omega t$ is the vector potential of the laser field.

To solve Eq. (2), we carry out the Henneberger unitary transformation to the oscillating frame [8]. Let

$$\Psi_{\rm f}^- = e^{-i\int^t d\tau\, V_{\rm L}(\tau)}\Phi = e^{-(i\boldsymbol{\alpha}\cdot\hat{\mathbf{P}}+U)}\Phi_{\rm f}^-, \tag{3}$$

with

$$\boldsymbol{\alpha} = \frac{1}{c}\int^t d\tau\, \mathbf{A}(\tau) = -\frac{\boldsymbol{\beta}}{\omega}, \qquad \boldsymbol{\beta} = \frac{1}{c}\int^{\varphi} \mathbf{A}(\varphi')d\varphi', \tag{4}$$

$$U = \int^t d\tau \frac{A^2(\tau)}{2c^2} = -\frac{1}{\omega}\int^{\varphi} d\varphi' \frac{A^2(\varphi')}{c^2} \equiv -\frac{1}{\omega}[U_1(\varphi) + \varphi U_{\rm p}], \tag{5}$$

where $U_{\rm p} = I/(4\omega^2)$ is the ponderomotive energy, I is the intensity, and $U_1(\varphi)$ is a periodic function in φ.

In the oscillating frame, $\Phi_{\rm f}^-$ is the wave function for an electron in an oscillating Coulomb center. For low-frequency laser fields, as is the case in the experiment of Smeenk *et al*. [1], the oscillating Coulomb center can be considered quasistatic, and therefore, $\Phi_{\rm f}^-$ is given approximately by a Coulomb scattering state wave function $\Psi_{{\rm A},\mathbf{p}}^-$,

$$\Phi_{\rm f}^- \approx \Psi_{{\rm A},\mathbf{p}}^- = \frac{e^{\pi a/2}\Gamma(1+ia)}{(2\pi)^{3/2}}\, {}_1F_1(-ia,1,-i(\mathbf{p}\cdot\mathbf{r} + pr)) \times e^{i\mathbf{p}\cdot\mathbf{r} - iE_{\rm p}t}, \tag{6}$$

where $E_{\rm p} = p^2/2$, $a = Z/p$, and Z is the effective atomic core charge. Substituting Eq. (6) into Eq. (3), then the final-state wave function $\Psi_{\rm f}^-$ is

$$\Psi_{\rm f}^- \approx e^{-i\int^t d\tau\, V_{\rm L}(\tau)}\Psi_{{\rm A},\mathbf{p}} \approx e^{-i(\boldsymbol{\alpha}\cdot\hat{\mathbf{P}}+U)}\Psi_{{\rm A},\mathbf{p}}^-. \tag{7}$$

As we see, embedded in the final-state wave function as given by Eq. (7) is a dependence on p_z. Moreover, it treats both the laser field and the Coulomb potential on equal footing and, therefore, provides the most accurate account of Coulomb effects in the final state. The recently observed low-energy structures [9] and the observed shifts in the two-dimensional momentum distributions in the polarization plane [10,11], which are due to Coulomb effects, can be accounted for by using the final-state wave function given by Eq. (7) [12,13]. The accurate representation of the Coulomb potential in the final state comes with a price. The analytical evaluation of

*titi@uwindsor.ca
†gdrake@uwindsor.ca

the transition amplitude given by Eq. (1) becomes more difficult. This is because the Coulomb scattering state wave function $\Psi^{-}_{\mathrm{A},\mathbf{p}}$ is not an eigenvector of the operator $e^{-i(\boldsymbol{\alpha}\cdot\hat{\mathbf{P}}+U)}$. We begin by writing $\Psi_{\mathrm{A},\mathbf{p}}(\mathbf{r}) = (2\pi)^{-3/2}\int d\mathbf{q}\, e^{i\mathbf{q}\cdot\mathbf{r}}\tilde{\Psi}_{\mathrm{A},\mathbf{p}}(\mathbf{q})$ and $\Phi_{\mathrm{i}}(\mathbf{r}) = (2\pi)^{-3/2}\int d\mathbf{q}\, e^{i\mathbf{q}\cdot\mathbf{r}}\tilde{\phi}_{\mathrm{i}}(\mathbf{q})$. Due to the transversality condition ($\mathbf{k}$ is perpendicular to both $\mathbf{A}$ and $\boldsymbol{\alpha}$), the plane wave $e^{i\mathbf{q}\cdot\mathbf{r}}$ is an eigenvector of V_{L} and $e^{-i\int^{t} dt' V_{\mathrm{L}}(t')}$. Using Eqs. (4) and (5) and the Fourier components introduced above, Eq. (1) reads

$$
\begin{aligned}
&(S-1)_{\mathrm{fi}} \\
&\quad = -i\int_{-\infty}^{\infty} dt \int d\mathbf{q}\int d\mathbf{q}'\int d\mathbf{r}\frac{e^{iE_{\mathrm{T}}t}}{(2\pi)^3}\tilde{\Psi}^{*}_{\mathrm{A},\mathbf{p}}(\mathbf{q})\tilde{\phi}_{\mathrm{i}}(\mathbf{q}') \\
&\qquad \times \exp\left[-i\frac{U_{\mathrm{p}}}{\omega}(\mathbf{k}\cdot\mathbf{r}-\omega t)\right]\exp\left\{-\frac{i}{\omega}[\boldsymbol{\beta}(\varphi)\cdot\mathbf{q}+U_1(\varphi)]\right\} \\
&\qquad \times V_{\mathrm{L}}(\mathbf{q}',\varphi)e^{i(\mathbf{q}'-\mathbf{q})\cdot\mathbf{r}}, \qquad (8)
\end{aligned}
$$

where $E_{\mathrm{T}} = E_{\mathrm{p}} + E_{\mathrm{B}}$ and E_{B} is the ground-state binding energy. Now, $\exp\{-\frac{i}{\omega}[\boldsymbol{\beta}(\varphi)\cdot\mathbf{q}+U_1(\varphi)]\}V_{\mathrm{L}}(\mathbf{q}',\varphi)$ is periodic in φ with a period 2π. Thus, we write $\exp\{-\frac{i}{\omega}[\boldsymbol{\beta}(\varphi)\cdot\mathbf{q}+U_1(\varphi)]\}V_{\mathrm{L}}(\mathbf{q}',\varphi) = \sum_n a_n(\mathbf{q},\mathbf{q}')\,e^{in\varphi}$ with the Fourier components $a_n(\mathbf{q},\mathbf{q}') = \frac{1}{2\pi}\int_0^{2\pi}\exp\{-\frac{i}{\omega}[\boldsymbol{\beta}(\varphi)\cdot\mathbf{q}+U_1(\varphi)] - in\varphi\}V_{\mathrm{L}}(\mathbf{q}',\varphi)d\varphi$. With the definitions $\Delta^{(n)} = n\omega - U_{\mathrm{p}}$ and $\tilde{\mathbf{k}}^{(n)} = \frac{1}{\omega}\Delta^{(n)}\mathbf{k}$, the expression for the transition probability then reads

$$
\begin{aligned}
(S-1)_{\mathrm{fi}} = -i\sum_n\int_{-\infty}^{\infty} dt\int d\mathbf{q}\int d\mathbf{q}'\int d\mathbf{r}\frac{e^{i(E_{\mathrm{T}}-\Delta^{(n)})t}}{(2\pi)^3} \\
\times\tilde{\Psi}^{*}_{\mathrm{A},\mathbf{p}}(\mathbf{q})\tilde{\phi}_{\mathrm{i}}(\mathbf{q}')a_n(\mathbf{q},\mathbf{q}')e^{i[\mathbf{q}'-\mathbf{q}+\tilde{\mathbf{k}}^{(n)}]\cdot\mathbf{r}}. \qquad (9)
\end{aligned}
$$

The temporal and spacial integrals yield the energy-conserving δ function $2\pi\delta(E_{\mathrm{T}}-\Delta^{(n)})$ and the linear momentum conserving δ function $(2\pi)^3\delta(\mathbf{q}-\mathbf{q}'-\tilde{\mathbf{k}}^{(n)})$, respectively. Using the transversality condition and integrating by parts gives $a_n(\mathbf{q}') = -\frac{\Delta^{(n)}}{2\pi}\int_0^{2\pi} d\varphi\,\exp\{-\frac{i}{\omega}[\boldsymbol{\beta}(\varphi)\cdot\mathbf{q}'+U_1(\varphi)+n\varphi]\}$. Thus, the expression for the transition amplitude becomes

$$
\begin{aligned}
(S-1)_{\mathrm{fi}} = -2\pi i\sum_n\delta(E_{\mathrm{T}}-\Delta^{(n)})\frac{\Delta^{(n)}}{2\pi}\int_0^{2\pi} d\varphi \\
\times\exp\left\{-\frac{i}{\omega}[U_1(\varphi)+n\varphi]\right\}\int d\mathbf{q}'\tilde{\Psi}^{*}_{\mathrm{A},\mathbf{p}}(\mathbf{q}'+\tilde{\mathbf{k}}^{(n)}) \\
\times\tilde{\phi}_{\mathrm{i}}(\mathbf{q}')e^{i\boldsymbol{\alpha}\cdot\mathbf{q}'}, \qquad (10)
\end{aligned}
$$

where we used $\boldsymbol{\alpha} = -\boldsymbol{\beta}/\omega$. Now, $\tilde{\Psi}_{\mathrm{A},\mathbf{p}}(\mathbf{q})$ is the Fourier transform of the Coulomb scattering state, which, as a limiting process, can be evaluated as a Nordsieck integral [14], thus, yielding

$$
\begin{aligned}
\tilde{\Psi}^{*}_{\mathrm{A},\mathbf{p}}(\mathbf{q}) = -\frac{\Gamma(1-ia)e^{\pi a/2}}{2\pi^2}\lim_{\lambda\to 0}\frac{\partial}{\partial\lambda}\frac{1}{(\mathbf{p}-\mathbf{q})^2+\lambda^2} \\
\times\left[\frac{\mathbf{q}^2-(p-i\lambda)^2}{(\mathbf{p}-\mathbf{q})^2+\lambda^2}\right]^{-ia} \qquad (11)
\end{aligned}
$$

evaluated at $\mathbf{q} = \mathbf{q}' + \tilde{\mathbf{k}}^{(n)}$. The value of the integral over $\mathbf{q}'$ in Eq. (10) is mainly determined by the poles of the integrand. The poles are $q' = |\mathbf{p}-\tilde{\mathbf{k}}^{(n)}| + i\lambda$ and $q' = iZ$. Moreover, due to the damping of the $e^{i\mathbf{q}'\cdot\boldsymbol{\alpha}}$ term in the integral, the contribution due to the pole $q' = |\mathbf{p}-\tilde{\mathbf{k}}^{(n)}| + i\lambda$ is larger than the pole $q' = iZ$. Furthermore, if we carry the process of differentiation with respect to λ, we get a leading term which is identified as a Dirac δ function, namely, $\lim_{\lambda\to 0}\frac{1}{\pi^2}\frac{\lambda}{[(\mathbf{p}-\mathbf{q})^2+\lambda^2]^2} = \delta(\mathbf{p}-\mathbf{q})$. Therefore, the value of the above integral is largely due to the pole $\mathbf{q}' = \mathbf{p}-\tilde{\mathbf{k}}^{(n)}$, and $\tilde{\phi}_{\mathrm{i}}(\mathbf{q}')$ is taken outside the integral and is evaluated at $\mathbf{q}' = \mathbf{p}-\tilde{\mathbf{k}}^{(n)}$. Consequently, it is easy to see that the integral over $\mathbf{q}'$ equals $(2\pi)^{3/2}\Psi^{(-)}_{\mathrm{A},\mathbf{p}}(\boldsymbol{\alpha})$. Therefore, Eq. (10) now reads

$$
\begin{aligned}
(S-1)_{\mathrm{fi}} = 2\pi i e^{\pi a/2}\Gamma(1+ia)\sum_n\delta(E_{\mathrm{T}}-\Delta^{(n)}) \\
\times\frac{\Delta^{(n)}}{2\pi}\tilde{\phi}_{\mathrm{i}}(\mathbf{p}-\mathbf{k}^{(n)})\int_0^{2\pi} d\varphi\, e^{i[\mathbf{p}\cdot\boldsymbol{\alpha}(\varphi)+U_1(\varphi)+n\varphi]} \\
\times{}_1F_1(-ia,1,-i[p\alpha(\varphi)+\mathbf{p}\cdot\boldsymbol{\alpha}(\varphi)]). \qquad (12)
\end{aligned}
$$

The probability amplitude as given by Eq. (12) is consistent with the simultaneous transfer of linear and angular momenta [12,13].

Smeenk *et al.* [1], on the basis of classical physics, obtained, for the net longitudinal momentum after the pulse has passed, $p_z = E_{\mathrm{p}}/c$. We interpret their result as coming from two contributions. The first is due to a constant magnetic-field Lorentz force (constant pulse envelope), representing the forward momentum due to radiation pressure on the photoelectron. The second contribution comes from the Lorentz force due to the gradient of the pulse envelope, which results in a negative force as the pulse passes over the electron. It removes part of the forward momentum due to radiation pressure and transfers it to the center of mass of the electron-ion system. The sum of both contributions gives a net $p_z = E_{\mathrm{p}}/c$. The results of our numerical calculations will prove this assertion. Of course, to compare the results of our numerical calculations with the experimental results of Smeenk*et al.* [1], the pulse envelope has to be taken into account via the space-time average over the focal volume. This focal volume averaging, as we see, does account for the Lorentz force due to the pulse envelope. In the ionization process by a circularly polarized light field, unlike the transfer of angular momentum, Coulomb effects for a first approximation can be ignored in the transfer of longitudinal momentum and are disregarded in our numerical calculations. To this end, using Eq. (12) and ignoring Coulomb effects, the ionization rate per unit of longitudinal momentum at a constant intensity is

$$
\frac{dW(I)}{dp_z} = \sum_{n=n_0}^{\infty}\frac{32Z^5\Delta^{(n)2}J_n^2\left[\frac{2}{\omega}\sqrt{U_{\mathrm{p}}\left(\Delta^{(n)}-E_{\mathrm{B}}-\frac{p_z^2}{2}\right)}\right]}{\left[Z^2+2(\Delta^{(n)}-E_{\mathrm{B}})+\frac{\Delta^{(n)2}}{c^2}-\frac{2}{c}\Delta^{(n)}p_z\right]^4}, \qquad (13)
$$

where n_0 is the minimum number of photons required for threshold ionization. Since dW/dp_z is not an even function of p_z, then $\int_{-\infty}^{\infty} dp_z\frac{dW}{dp_z}p_z \neq 0$, implying a net longitudinal momentum transfer (see Fig. 1).

For the case of ionization by a linearly polarized laser, the Bessel function in Eq. (13) is replaced by a generalized Bessel function. This implies that linearly and circularly polarized pulses will transfer very different longitudinal momenta to the photoelectron. (In circular polarization, photoelectrons are

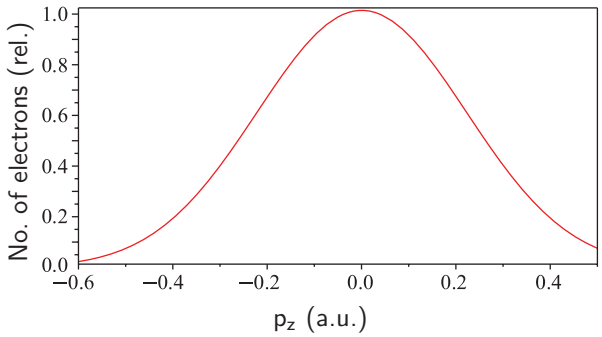

FIG. 1. (Color online) Number of electrons, in relative units, according to Eq. (13) for Ne in circularly polarized light at 800 nm and $I = 8 \times 10^{14}$ W/cm^2. The curve resembles a Gaussian distribution with a small offset of the center due to photon linear momentum (cf. Fig. 1 of Smeenk *et al.* [1]).

more energetic, $E_p \approx U_p$, than those of linear polarization where E_p is in the vicinity of the threshold.)

In the following, we confirm that the net longitudinal momentum transferred $p_z = E_p/c$. From Eq. (12), the ionization rate per unit energy to detect an electron, at constant intensity, is

$$\frac{d\bar{W}(I)}{dE_p} = 32Z^5 \sum_{n=n_0}^{\infty} \delta(E_T - \Delta^{(n)})\sqrt{2E_p} \int_0^{\pi} d\theta \times \frac{\sin\theta \Delta^{(n)2} J_n^2\left(\frac{2}{\omega}\sqrt{U_p E_p}\sin\theta\right)}{\left[Z^2 + 2E_p + \frac{1}{c^2}\Delta^{(n)2} - \frac{2}{c}\Delta^{(n)}\sqrt{2E_p}\cos\theta\right]^4}, \tag{14}$$

where θ is the angle between $\mathbf{p}$ and $\mathbf{k}$ and $U_p = \frac{I}{4\omega^2}$. For a Gaussian pulse envelope, as in the case of the experiment of Smeenk *et al.* [1], the intensity distribution within the focal volume is [15]

$$\frac{I(\rho,z)}{I_0} = \left(\frac{\omega_0}{\omega(z)}\right)^2 \exp[-4\ln(2)(z-ct)^2/(c^2\tau^2) - 2\rho^2/\omega(z)^2], \tag{15}$$

where $\omega(z) = \omega_0[1 + (z/z_0)^2]^{1/2}$, $\omega_0 = \sqrt{\lambda z_0/\pi}$ is the Rayleigh range, and τ is the temporal full width at half maximum in intensity. The focal volume consists of surfaces of constant intensity. The differential volume element is a shell between two surfaces of constant intensity I and $I + dI$. Atoms lying within a given differential volume element are ionized at a constant intensity I. Then, within the focal volume, the total number of electrons generated per unit of energy is

$$\frac{dN}{dE_p} = 2\pi\tau\rho_d z_0 \omega_0^2 \int_0^{I_0} \frac{dI}{I^{5/2}}\sqrt{I_0 - I}\frac{d\bar{W}(I)}{dE_p} \times \int_0^1 d\eta[I + (I_0 - I)\eta^2]\left[\ln\frac{I_0}{I + (I_0 - I)\eta^2}\right]^{1/2}, \tag{16}$$

where ρ_d is the atomic density. If $N_t = \int_0^{\infty} dE_p \frac{dN}{dE_p}$ denotes the total number of electrons with energy $E_p \geqslant 0$, then the

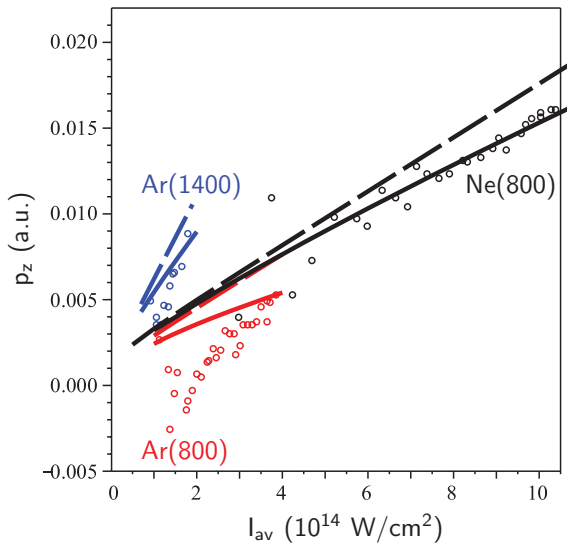

FIG. 2. (Color online) Solid curves: the results of theoretical calculations with focal averaging and dashed curves: without focal averaging superimposed on the experimental data (circles) of Smeenk *et al.* [1]. The upper: blue, middle: black, and lower: red curves are for Ar at 1400 nm, Ne at 800 nm, and Ar at 800 nm, respectively.

average kinetic energy of electrons is

$$\bar{E}_p = \frac{1}{N_t}\int_0^{\infty} dE_p E_p \frac{dN}{dE_p} = \frac{\int_0^{\infty} dE_p E_p \frac{dN}{dE_p}}{\int_0^{\infty} dE_p \frac{dN}{dE_p}}, \tag{17}$$

where $\frac{dN}{dE_p}$ is given by Eqs. (16) and (14).

In Fig. 2, the results of the theoretical calculations for p_z versus the average intensity at ionization I_{av} are superimposed on the experimental data of Smeenk *et al.* [1]. The values used for the binding energy are 21.5645 eV for Ne and 15.7596 eV for Ar. The dashed curves are the results of the calculations without focal averaging. In this case, it is clear that the dashed curves are well above the experimental data. This implies that the Lorentz force due to a constant pulse envelope alone does not account for the experimental data. The solid curves are the results of the calculations, including the focal volume averaging.

The agreement between theory and experiment is satisfactory in the case of Ar at 1400 nm (upper curve) and Ne at 800 mn (middle curve), but the experimental points fall progressively below theory for Ar at 800 nm (lower curve), especially in the intensity range of 1×10^{14} to 1.5×10^{14} W/cm^2 where the experimental data exhibit a negative p_z. Thus, we conclude from the first two comparisons that the focal volume averaging accounts for the Lorentz force due to the gradient of the pulse envelope, producing a negative force counteracting the force due to a constant envelope. We attribute the poor agreement in the case of Ar(800) to Coulomb effects, which are neglected in the numerical calculations. As discussed by Reiss [7], Coulomb effects can be neglected provided that the intensity parameter $z_1 = 2U_p/E_B$ satisfies the condition $z_1 > 1$. The actual values at the lowest intensity $I = 1 \times 10^{14}$ W/cm^2 in Fig. 2 are $z_1 = 2.322$ for Ar(1400) where agreement is good but $z_1 = 0.758$ for Ar(800) where agreement is poor. For Ne(800), $z_1 = 1.66$ at the lowest

measured intensity point of 3×10^{14} W/cm^2 in harmony with satisfactory agreement at higher intensities. However, z_1 would decrease linearly with intensity to only $z_1 = 0.553$ at $I = 1 \times 10^{14}$ W/cm^2. One would, therefore, expect to see similarly significant deviations for Ne(800) at low intensities. There may be some evidence for this at the low-intensity end in Fig. 2. Further measurements for Ne(800) in the low-intensity range would be very useful.

The results for Ar(800), thus, demonstrate the influence of Coulomb effects at low intensities and especially, the negative values of p_z. The inclusion of Coulomb effects in the numerical calculations would account for the attractive Coulomb force along the z direction and would explain negative values of p_z. Similar to the low-energy structures recently observed in ionization by linearly polarized light [9], we believe that the experimental data for Ar(800) at low intensities provide evidence of Coulomb effects in ionization by circularly polarized light. This will be investigated further in a future paper.

In conclusion, we have presented a quantum formulation for the transfer of longitudinal momentum in the ionization process. Nondipole effects account for the Lorentz magnetic force due to a constant envelope, thus, giving rise to the radiation pressure, which is the essential mechanism for the transfer of longitudinal momentum. However, this by itself is not sufficient to account for the experimental data. At high intensities, the combined effect of both the nondipole corrections and the pulse envelope accurately account for the experimental data. In this limit, we have demonstrated the validity of the assertion that $p_z = E_p/c$. At low intensities, where Coulomb effects cannot be ignored, p_z is evidently reduced by the work performed against the attractive Coulomb force along the z axis and may even become negative.

We are grateful to Dr. Paul Corkum for drawing our attention to this problem. Research support by the Natural Sciences and Engineering Research Council of Canada, SHARCNET, and Compute/Calcul Canada is gratefully acknowledged.

[1] C. T. L. Smeenk, L. Arissian, B. Zhou, A. Mysyrowicz, D. M. Villeneuve, A. Staudte, and P. B. Corkum, Phys. Rev. Lett. **106**, 193002 (2011).
[2] G. Marx, Nature (London) **211**, 22 (1966).
[3] S. Gigan, H. R. Bohm, M. Paternostro, F. Blaser, G. Langer, J. B. Hertzberg, K. C. Schwab, D. Bauerle, M. Aspelmeyer, and A. Zeilinger, Nature (London) **444**, 67 (2006).
[4] C. C. Cheng, E. M. Wright, and J. V. Moloney, Phys. Rev. Lett. **87**, 213001 (2001).
[5] C. D. Amico, A. Hourad, S. Akturk, Y. T. Tikhonchuk, and A. Mysyrwicz, New J. Phys. **10**, 013015 (2008).
[6] P. Sprangle, J. R. Penano, B. Hafizi, and C. A. Kapetanakos, Phys. Rev. E **69**, 066415 (2004).
[7] H. R. Reiss, Phys. Rev. A **22**, 1786 (1980).
[8] W. C. Henneberger, Phys. Rev. Lett. **21**, 838 (1968).
[9] C. Blaga, F. Catoire, P. Colisimo, G. Paulus, H. Muller, P. Agostini, and L. Dimauro, Nat. Phys. **5**, 335 (2008).
[10] C. P. J. Martiny, M. Abu-Samha, and L. B. Madsen, J. Phys. B **42**, 161001 (2009).
[11] P. Eckle, A. N. Pleiffer, C. Cirelli, A. Slaudte, R. Dörner, H. G. Muller, M. Büttiker, and U. Keller, Science **322**, 1525 (2008).
[12] A. S. Titi, Ph.D. dissertation, University of Windsor, 2011.
[13] A. S. Titi and G. W. F. Drake (unpublished).
[14] A. Nordsieck, Phys. Rev. **93**, 785 (1954).
[15] R. Kopold, W. Becker, M. Kleber, and G. G. Paulus, J. Phys. B **35**, 217 (2002).